

# Transfer of aligned single crystal silicon nanowires to transparent substrates

Shu-Chia Shiu, Chieh-Yu Hsiao, Cha-Hsin Chao and Shih-Che Hung

Graduate Institute of Photonics and Optoelectronics, National Taiwan University, Taipei, Taiwan,  
10617 R.O.C

Ching-Fuh Lin

Graduate Institute of Photonics and Optoelectronics, Graduate Institute of Electronics Engineering  
and Department of Electrical Engineering, National Taiwan University, Taipei, Taiwan, 10617  
R.O.C.

Corresponding author: Ching-Fuh Lin, Tel: 886-2-3366 3540; Fax: 886-2-2364 2603; E-mail address:  
[cflin@cc.ee.ntu.edu.tw](mailto:cflin@cc.ee.ntu.edu.tw)

## ABSTRACT

We demonstrate the method of transferring aligned single crystal silicon nanowires (SiNWs) to transparent substrate. The alignment of the transferred nanowires is almost identical to the original one. The density of the transferred SiNWs can achieve  $3 \times 10^7$  nanowires/mm<sup>2</sup>. The low temperature fabrication processes are compatible for a wide range of substrates. The transmission coefficient below 10 % at a wide bandwidth, 400-1100 nm, was found in the transferred SiNWs. The high dense aligned SiNWs are promising for future photovoltaic applications.

**Keyword:** silicon, nanowires, transfer, transparent, aligned, low temperature, electroless, transmission spectrum, SEM, bending stress.

## 1. Introduction

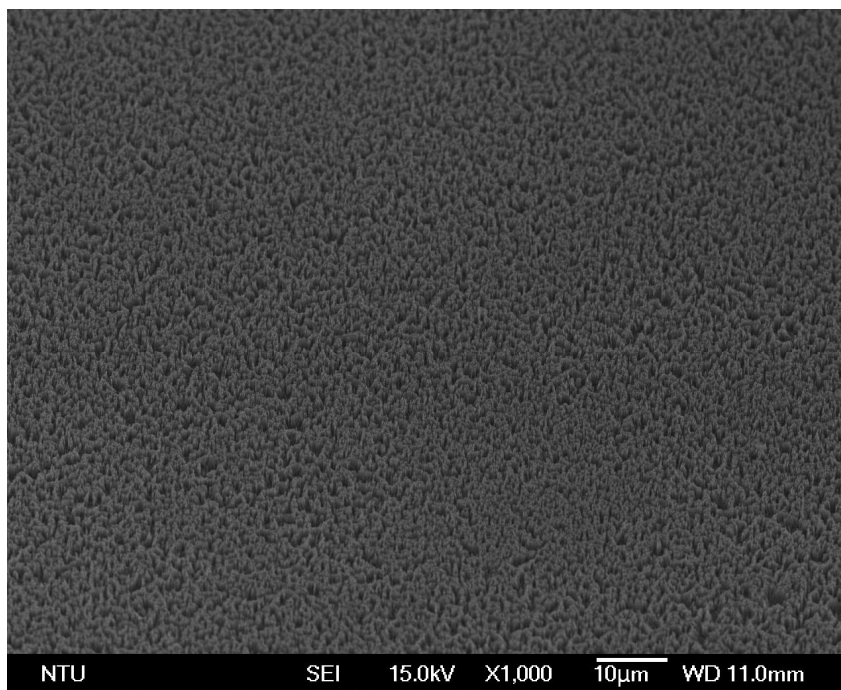
In recent years, applications of electronic devices on glass and plastic substrates have attracted a lot of attention. Many methods have been developed to directly fabricate high performance semiconductor electronic devices on these substrates, including wet transfer<sup>1</sup>, contact print<sup>2</sup>, and self-assembled<sup>3</sup> methods. Among these methods, transfer of semiconductor nanowires attracted considerable attention owing to their novel properties resulting from their unique geometry.<sup>4-9</sup> Semiconductor nanowires can be made as active device elements and passive interconnects simultaneously. Besides, ultra-large surface-to-volume ratio and quantum confinement effect made a wide range of applications, including field-effect transistors<sup>10</sup>, light emitting diodes<sup>11</sup>, lasers<sup>12</sup>, photo-detectors<sup>13</sup>, bio/chemical sensors<sup>14, 15</sup>, photovoltaic applications<sup>16-18</sup> and thermoelectric devices<sup>19, 20</sup>. Some researchers have successfully demonstrated parallel nanowire devices on the plastic substrates. However, the density of nanowire devices was restricted by the architecture of the parallel-aligned nanowires. In comparison to the parallel nanowire devices on the plastic substrates, the architecture of vertically aligned nanowires can achieve high dense electronic devices, and are promising for photovoltaic applications, and field emission display applications. Yet, to date, vertically-aligned nanowires on glass or plastic substrates have not been demonstrated.

In this work, we presented a method of transfer of vertically-aligned single crystalline silicon nanowires (SiNWs). The advance of Si technology makes Si the most important materials for electronics industry. As the Moore's law pushes the feature size down to the nanometer scale, SiNWs continues to attract significant attention because they have potential applications even beyond electronics. The mature technique of silicon USLI made silicon nanowire promising to be integrated on plastic or glass substrates. SiNWs can be fabricated using chemical vapor deposition (CVD)<sup>21</sup>, laser ablation<sup>22</sup>, and solution methods<sup>23</sup>. High-temperature hazardous silicon precursors, complex equipment, and other rigorous conditions are often required. Our method is based on a simple bonding process that enables the direct transfer of vertically-aligned SiNWs from a silicon wafer to a receiver substrate. The process is compatible with a wide range of receiver substrates, including glass and plastics.

## 2. Synthesis of silicon nanowires

SiNWs used in transfer processes were prepared by an aqueous electroless etching (EE) method, as the method can synthesize wafer-scale vertically-aligned SiNWs. The working principle of synthesizing SiNWs is the galvanic displacement reaction; that is, the reduction of metal ions (cathodic process) and the oxidation of Si atoms (anodic process) occur simultaneously at the Si surface<sup>24</sup>. An n-type 1–10 ohm-cm Si (100) wafer was used to synthesize SiNWs in an aqueous solution of AgNO<sub>3</sub> and HF acid. The solution concentration of AgNO<sub>3</sub> and HF are 0.023 and 5.6 molL<sup>-1</sup>, respectively. The mechanism based on Ag-enhanced electroless etching of silicon wafer was described in the following. First, Ag<sup>+</sup> ions in the vicinity of the silicon surface capture electrons from the Si valence band (VB) and oxidizing the surrounding lattice, which is subsequently etched by HF. The energy levels of the Ag<sup>+</sup>/Ag system lie well below the Si VB edge, so they more likely interact with the VB bonding electrons of silicon and active kinetics are expected for the electron-capture process. Ag<sup>+</sup> ions are deposited in the form of metallic Ag nuclei on a nanoscopic scale on the wafer surface, thus delimiting the spatial extent of the oxidation and etching process. Further reduction of Ag<sup>+</sup> occurs on the nanoparticles, not the Si wafer, which becomes the active cathode by electron transfer from the underlying wafer. The arrays of SiNWs will be formed vertically and covered large areas on the Si wafer. Then, the arrays of SiNWs were washed in a concentrated nitric acid bath to remove all Ag dendritic structures from the nanowire surfaces. Finally, the SiNWs were immersed in the buffer-oxide-etch to remove oxide layer on the SiNWs.

SiNWs arrays prepared by this method were aligned and covered the area up to the wafer size. The length of these SiNWs could be adjusted by the etching time. Figure 1 shows the scanning electron microscopy (SEM) images of the cross-section of SiNWs arrays at the etching time, 20, 30, and 40 min. The length of SiNWs etched with the above etching time was 5.42, 7.08, and 11.32  $\mu\text{m}$ , respectively. These SiNWs were 10 - 300 nm in diameter. The top morphology of arrays SiNWs was greatly influenced by the etching time of the Si wafer in the AgNO<sub>3</sub> - HF solution. At etching time, 20 and 30 min, SiNWs were vertically aligned on the Si wafer as shown in the figure 1(a). However, at the etching time, 40 min, the top morphology of SiNWs formed large nanowire bundles as shown in figure 1(b). The size of the SiNWs bundles was about 3-5  $\mu\text{m}$ , which was much larger than the diameter of SiNWs. We thought that the morphology of very long SiNWs was influenced seriously by the surface tension of the solution used in synthesizing SiNWs. The morphology of the SiNWs greatly influenced the transfer of SiNWs, and the reason will be discussed later.



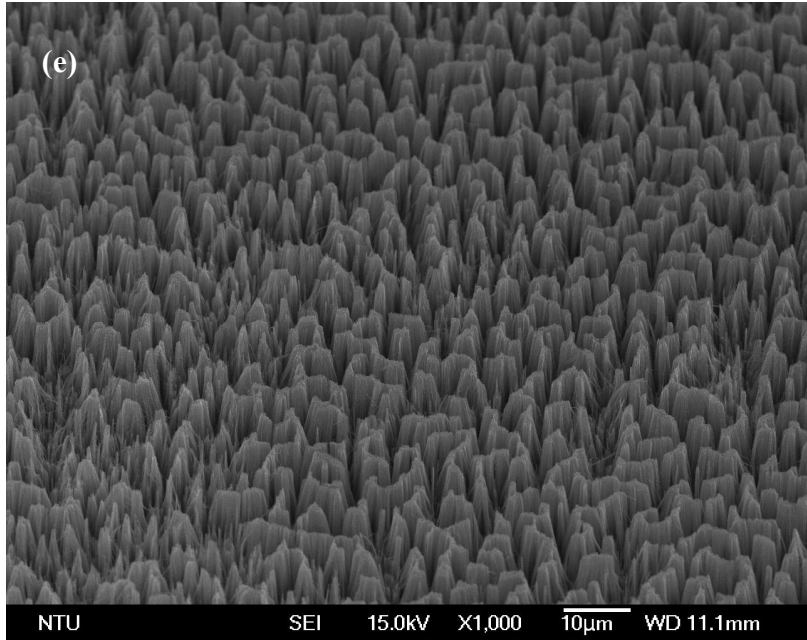


Fig. 1 The scanning electron microscopy image of the as-etched silicon nanowires. Figure (a) and (b) are the top view of the SEM image of as-etched SiNWs with length, 5µm and 11µm.

### 3. Transfer of silicon nanowires

The transfer method of SiNWs involves direct bonding of Si wafer, consisting of vertically aligned EE SiNWs, on top of a receiver substrate coated with PMMA [poly(methyl methacrylate)]. The schematic of the process flow for transfer of SiNWs is shown in figure 2. The solution of PMMA/chloroform ( $\text{CHCl}_3$ ) were prepared by weight in concentrations of 2.5 wt.%. The PMMA solution was spin coated on the receiver substrate. The thickness of the PMMA thin film was 390 nm. In the bonding step of transfer method, the PMMA were first heated to 215 °C, above the glass transition temperature of PMMA, 105 °C. The Si wafer with SiNWs was then pressed against the receiver substrate and held there until the temperature dropped below the PMMA's glass transition temperature. Various pressures were tested and it was found that the pressure influenced the density of the transferred SiNWs. During the bonding process, SiNWs were inserted into the PMMA thin film and anchored on the PMMA film. Finally, a gentle instant force was treated on the edge of the host wafer, and the SiNWs on the host wafer were cleaved. The vertically aligned SiNWs were transferred onto the receiver substrate. Because the transfer process was carried out at low temperature, a wide range of materials of receiver substrate could be used.

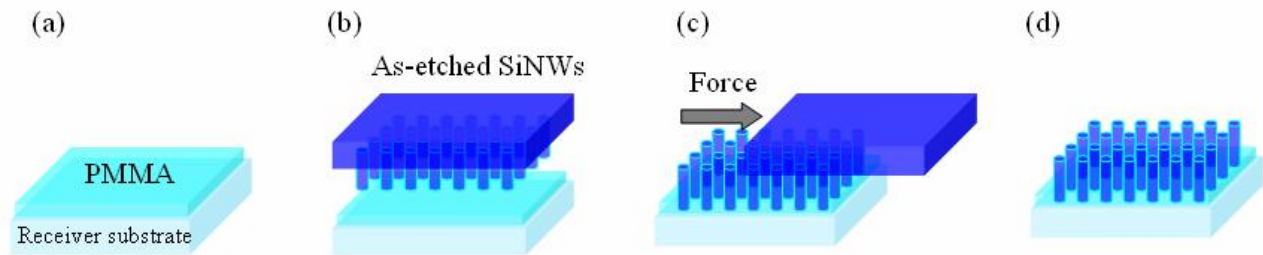


Fig. 2 Schematic of the method of transferring silicon nanowires onto receiver substrate.

### 4. Result and discussion

The scanning electron microscopy (SEM) images of transferred SiNWs on a receiver substrate are shown in Figure 3 (a), clearly demonstrating vertically-aligned SiNW films. The bonding pressure in the transfer process was about 8.78 kg/cm<sup>2</sup>. The SiNWs with length of 5.42 µm were transferred successfully onto the receiver substrates. The top-view SEM image shows that the density of transferred SiNWs is about  $1 \times 10^6$  nanowires/mm<sup>2</sup>. The density is significantly

lower than that of original SiNWs. This result indicated that the pressure in the bonding process was not high enough. The length of the inserted SiNWs in PMMA was less than 100 nm as shown in figure 3 (b). This can not make the SiNWs be tightly bonded on the PMMA film. Therefore, the SiNWs could be removed easily from the receiver substrate. Under the same bonding pressure, we attempted to transfer SiNWs with length of 11.32  $\mu\text{m}$  onto the receiver substrate. However, little SiNWs were transferred onto the receiver substrate. Instead, many holes and cracks formed on the PMMA film, and the size was about 1 – 10  $\mu\text{m}$ . The size of the holes and cracks was similar to that of the bundles of SiNWs as shown in figure 2. It is suggested that individual SiNWs in the SiNWs bundles were not bonded to the PMMA film. Therefore, the SiNWs can not be transferred onto receiver substrate, and holes and cracks formed on the PMMA film.

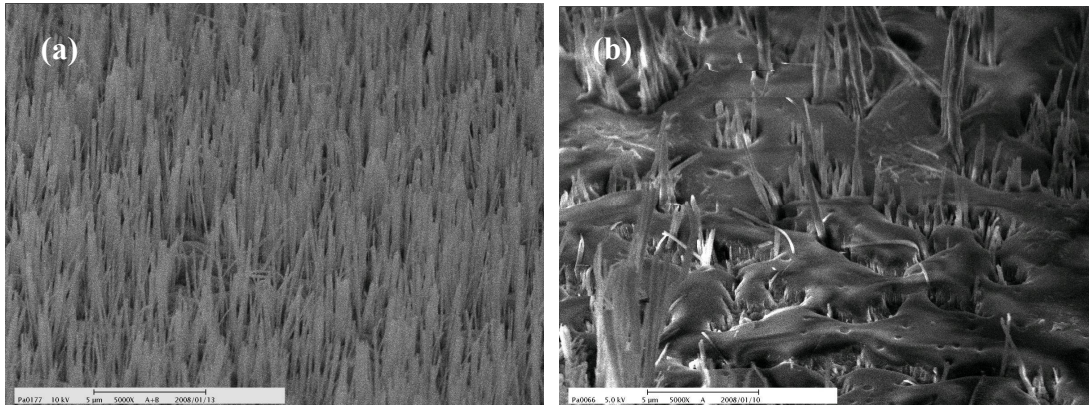


Fig. 3 The SEM image of the transferred SiNWs. (a) 5  $\mu\text{m}$  SiNWs were transferred. (b) 11  $\mu\text{m}$  SiNWs were transferred.

In order to increase the density of the transferred SiNWs on the receiver substrate, we increased the bonding pressure to 55  $\text{kg}/\text{cm}^2$  in the bonding process. The density of transferred SiNWs with a length of 5.42  $\mu\text{m}$  increased to  $3 \times 10^7$  nanowires/ $\text{mm}^2$ , as shown in the figure 4(a). Most transferred SiNWs were vertically aligned on the receiver substrate as the original ones. The length of the inserted SiNWs in PMMA increased to 300 nm, which is much longer than that under the pressure, 8.78  $\text{kg}/\text{cm}^2$ . This caused that individual SiNWs could be tightly bonded on the PMMA film even though the original SiNWs formed SiNWs bundles. Therefore, the SiNWs with length 11.32  $\mu\text{m}$  can also be transferred successfully under this condition, as shown in figure 4(b). The transferred SiNWs did not form SiNW bundles in comparison to the original ones. Most SiNWs can be cleaved and transferred on the PMMA film when the instant force was treated on the side of original Si wafer in the transfer process. Therefore, the low temperature processes can be used on the glass substrate. In addition, the transfer method did not influenced by the material of the receiver substrate or the crystal orientation, so vertically-aligned architecture of SiNW did not changed after transferring onto glass substrates.

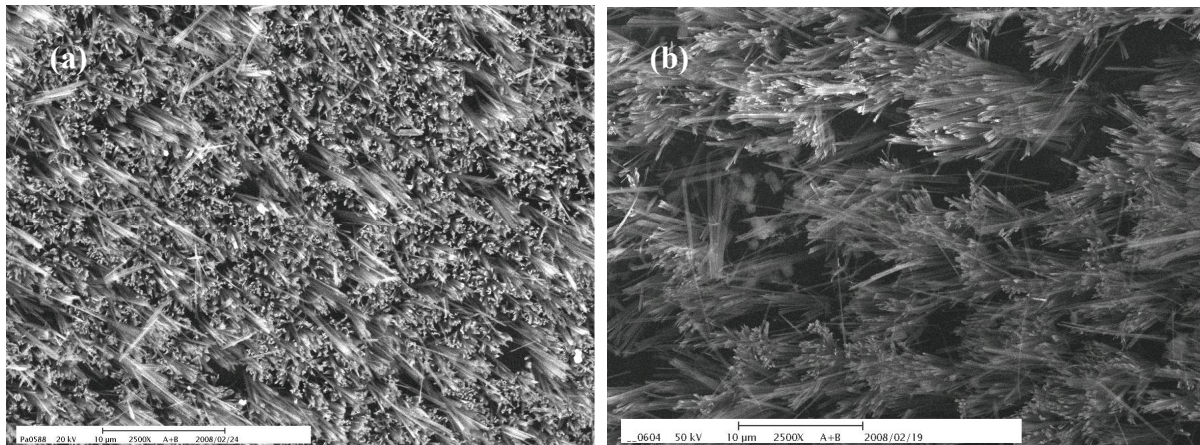


Fig. 4 The SEM image of the transferred SiNWs with a bonding pressure, 55  $\text{kg}/\text{cm}^2$ .

One of the reasons that the transfer of vertically aligned SiNWs was demonstrated successfully is due to the contact area between the SiNWs and the PMMA film. Ultra-large surface area of SiNWs made the transfer method success. As illustrating in figure 5, the SiNWs will be inserted into the PMMA film when a pressure was treated on the host substrate during the bonding process. The PMMA wrapped round the SiNWs. The contact area between the SiNWs and the PMMA film will be larger as the depth of the SiNWs inserting into PMMA film is deeper. However, the contact area between the SiNWs and the host substrate is much smaller than that between the SiNWs and the PMMA film. The contact area is equal to the diameter of the SiNWs. Therefore, when the force is treated on the edge of the host substrate, SiNWs will be cleaved at the ends of SiNWs close to the host substrate, but not close to the PMMA film.

The inserting depth of SiNWs also influenced the transfer processes, when the SiNWs formed bundles. As shown in figure 1(b), large SiNW bundles formed. This kind of SiNWs could not be transferred successfully onto the receiver substrate under the bonding pressure,  $8.78 \text{ kg/cm}^2$ . This is because the PMMA can not flow into the bundles of SiNWs. The phenomenon was illustrated in figure 5(a). At the end of the SiNW bundles, SiNWs will contact each other, and no space between SiNWs can be filled by PMMA. Some SiNWs can not be bonded in the PMMA film. Therefore, the bundles of SiNWs can not be transferred. However, as the bonding pressure was increased, the bundles of SiNWs can be transferred successfully as shown in figure 4(b). The inserting depth of SiNWs in PMMA increased as the bonding pressure increased. Then, there was space between SiNWs, and PMMA can flow into bundles of SiNWs as shown in figure 5(b). This caused that the bundles of SiNWs can also be bonded tightly in the PMMA film, and made the bundles of SiNWs be transferred successfully.

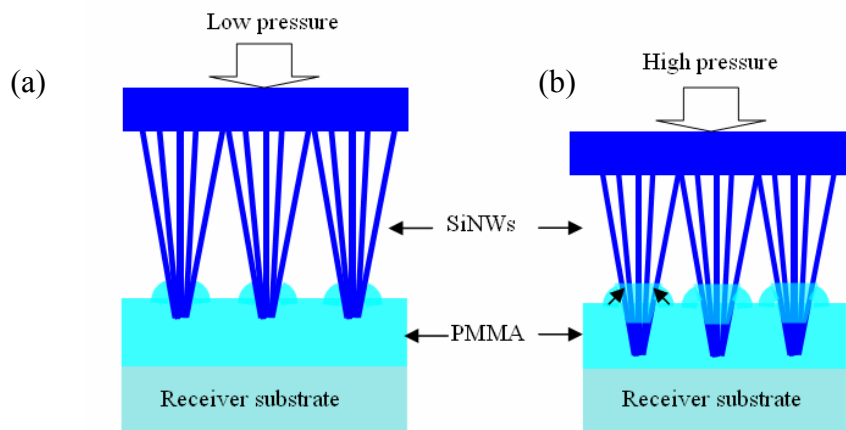


Fig. 5 The schematic of bonding the bundles of SiNWs under different pressure. (a) low pressure condition. (b) high pressure condition.

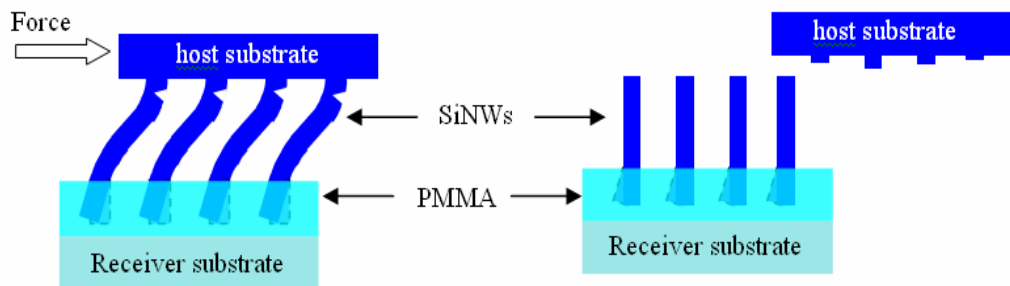


Fig. 6 The schematic of the mechanism of the transferring SiNWs.

The second reason is due to the different extent of the bending stress of the ends of SiNWs close to the side of the host substrate and the PMMA film. The maximum bending stress of SiNWs has been studied. The self-welded SiNWs could withstand a maximum bending stress in the range of 210–830 MPa, which also depended on the nanowire diameter and loading conditions<sup>24</sup>. The beam broke close to the loading point, rather than at the self-welded junction, indicating the excellent bond strength of the self-welded junction. In our transfer method, the SiNWs will be bent by the force treated on the edge of the host material. The bending of SiNWs can be illustrated as figure 6. The bending of SiNWs close to the host substrate will be more serious than that close to the PMMA film. The serious bending stress causes the SiNWs to be cleaved along the crystal planes of SiNWs close to the host substrate. This is because the PMMA has a much lower elastic modulus than that of silicon and the excellent bond strength of PMMA film. The bending stress of SiNWs near the side of the PMMA will be relaxed. After being cleaved from host substrate, SiNWs will return to the original vertically-aligned architecture. Therefore, the SiNWs can be cleaved at the side of the host substrate and vertically aligned on the receiver substrate.

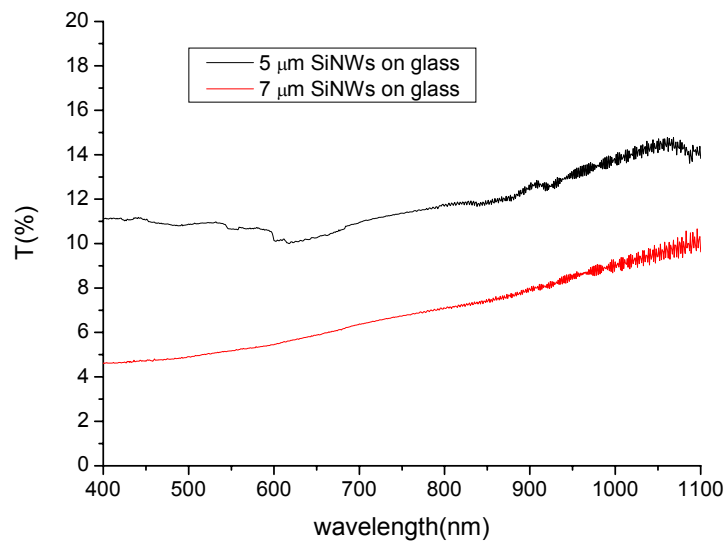


Fig. 7 The transmission spectrum of the transferred SiNWs on the glass substrate.

The reduction of optical loss is one of the important factors in obtaining high-efficiency Si solar cells. To achieve this goal, the top surface of the solar cells is generally texturized or covered with an antireflection coating (ARC). It is well known that porous silicon (PSi) can reduce the reflectance to 5.8% in the 400-1000 nm wavelength range and therefore can replace other surface-textured microstructure and antireflection coatings. Vertically-aligned SiNWs have been expected to have further improved optical characteristics compared to planar materials<sup>18</sup>. The optical reflectance of a typical SiNWs has been extensively studied. The results showed that the reflection of light is significantly reduced. The SiNW arrays could intensively suppress the reflection drastically over a wide spectral bandwidth ranging from 300 to 1000 nm. The reflectance about 1.4% or much less over the range of 300-600 nm for the arrays on Si substrates has been found<sup>26</sup>. However, the transmission spectrum of the vertically-aligned SiNWs has not been studied, owing to the difficulties to fabricate SiNWs on transparent substrate. Here, we can study the transmission properties of vertically-aligned SiNWs on the glass substrate by using the novel transfer method. Figure 7 shows the optical transmission spectrum of vertically-aligned SiNWs. The SiNWs shows weak transmission over the wide spectral bandwidth of 400–1000 nm. Note that the transmission of 7 μm SiNWs array is only 10 % or less in the range of 400–1000 nm. The remarkably low transmission is attributable to the ultrahigh surface area and subwavelength structured surface. Besides of significant reduction of reflection coefficient, the vertically-aligned transferred SiNWs on glass has low transmission coefficient found in this work.

## 5. Conclusion

In this paper, we demonstrated the transfer of aligned single crystal silicon nanowires on the transparent substrate successfully. The low temperature fabrication processes are suitable for photovoltaic applications on glass or plastic substrates. The silicon nanowires were first fabricated on a silicon wafer in the metal ionic HF solution at room temperature by selective etching of the silicon wafer. The PMMA was deposited on ITO glass by spin coating method. Then, the silicon nanowires were pressed upon the PMMA thin film at the temperature of 215 °C. Finally, the silicon substrate was removed and the silicon nanowires were transferred onto the PMMA thin film. The alignment of the transferred nanowires is almost identical to the original one. The length of silicon nanowires is about 4 μm and the width is about 100 nm on PMMA thin film. For photovoltaic applications, nanowire materials with significant high optical absorption coefficient have attracted much attention. The low transmission coefficient was observed on the transferred SiNWs.

## Reference

1. D. Whang, S. Jin, Y. Wu, and C. M. Lieber, "Large-Scale Hierarchical Organization of Nanowire Arrays for Integrated Nanosystems," *Nano Lett.* **3**, pp.1255-1259, 2003.
2. Z. Fan, J. C. Ho, Z. A. Jacobson, R. Yerushalmi, R. L. Alley, H. Razavi, and A. Javey, "Wafer-Scale Assembly of Highly Ordered Semiconductor Nanowire Arrays by Contact Printing," *Nano Lett.* **8**, pp.20-25, 2008.
3. S. A. Stauth and B. A. Parviz, "Self-assembled single-crystal silicon circuits on plastic," *PNAS* **103**, pp.13922-13927, 2006.
4. M. C. Mcalpine, H. Ahmad, D. Wang, and J. R. Heath, "Highly ordered nanowire arrays on plastic substrates for ultrasensitive flexible chemical sensors," *Nature* **6**, pp.379-384, 2007.
5. M. C. Mcalpine, R. S. Friedman, and C. M. Lieber, "High-Performance Nanowire Electronics and Photonics and Nanoscale Patterning on Flexible Plastic Substrates," *Proceedings of the IEEE* **93**, pp.1357-1363, 2005
6. Kook-Nyung Lee, Suk-Won Jung, Won-Hyo Kim, Min-Ho Lee, Kyu-Sik Shin and Woo-Kyeong Seong, "Well controlled assembly of silicon nanowires by nanowire transfer method," *Nanotechnology* **18**, 445302 (7pp), 2007.
7. Y. Huang, X. Duan, Q. Wei, C. M. Lieber, "Directed Assembly of One-Dimensional Nanostructures into Functional Networks," *Science* **291**, pp.630-633, 2001.
8. A. Javey, S. Nam, R. S. Friedman, H. Yan, and C. M. Lieber, "Layer-by-Layer Assembly of Nanowires for Three-Dimensional, Multifunctional Electronics," *Nano Lett.* **7**, pp.773-777, 2007.
9. N. A. Melosh, A. Boukai, F. Diana, B. Gerardot, A. Badolato, P. M. Petroff, J. R. Heath, "Ultrahigh-Density Nanowire Lattices and Circuits," *Science* **300**, pp.112-115, 2003.
10. J. Goldberger, A. I. Hochbaum, R. Fan, and P. Yang, "Silicon Vertically Integrated Nanowire Field Effect Transistors," *Nano Lett.* **6**, pp.973-977, 2006.
11. A. Nadarajah, R. C. Word, J. Meiss, and R. Konenkamp, "Flexible Inorganic Nanowire Light-Emitting Diode," *Nano Lett.* **8**, pp.534-537, 2008.
12. S. Gradečak, F. Qian, Y. Li, Hong-Gyu Park, and C. M. Lieber, "GaN nanowire lasers with low lasing thresholds," *Appl. Phys. Lett.* **87**, pp.173111, 2005.
13. C. Soci, A. Zhang, B. Xiang, S. A. Dayeh, D. P. R. Aplin, J. Park, X. Y. Bao, Y. H. Lo, and D. Wang, "ZnO Nanowire UV Photodetectors with High Internal Gain," *Nano Lett.* **7**, pp.1003-1009, 2007.
14. U. Cvelbar, K. Ostrikov, A. Drenik, and M. Mozetic, "Nanowire sensor response to reactive gas environment," *Appl. Phys. Lett.* **92**, pp.133505, 2008.
15. X. Wang, and C. S. Ozkan, "Multisegment Nanowire Sensors for the Detection of DNA Molecules," *Nano Lett.* **8**, pp.398-404, 2008.
16. B. Tian, X. Zheng, T. J. Kempa, Y. Fang, N. Yu, G. Yu, J. Huang, and C. M. Lieber, "Coaxial silicon nanowires as solar cells and nanoelectronic power sources," *Nature* **449**, pp.885-889, 2007.
17. Th. Stelzner, M. Pietsch, G. Andra, F. Falk, E. Ose and S. Christiansen, "Silicon nanowire-based solar cells," *Nanotechnology* **19**, pp.295203, 2008.
18. L. Tsakalacos, J. Balch, J. Fronheiser, B. A. Korevaar, O. Sulima, and J. Rand, "Silicon nanowire solar cells," *Appl. Phys. Lett.* **91**, pp.233117, 2007.
19. A. I. Hochbaum, R. Chen, R. D. Delgado, W. Liang, E. C. Garnett, M. Najarian, A. Majumdar, and P. Yang, "Enhanced thermoelectric performance of rough silicon nanowires," *Nature* **451**, pp.163-167, 2007.
20. A. I. Boukai, Y. Bunimovich, J. Tahir-Kheli, J. Yu, W. A. Goddard III & J. R. Heath, "Silicon nanowires as efficient thermoelectric materials," *Nature* **451**, pp.168-171, 2007.

21. Y. Cui, Lincoln J. Lauhon, M. S. Gudixsen, J. Wang, "Diameter-controlled synthesis of single-crystal silicon nanowires," *Appl. Phys. Lett.* **78**, pp.2214-2216, 2001.
22. A. M. Morales and C. M. Lieber, "A Laser Ablation Method for the Synthesis of Crystalline Semiconductor Nanowires," *Science* **279**, pp.208-211, 1998.
23. J. D. Holmes, K. P. Johnston, R. Christopher Doty, B. A. Korgel, "Control of Thickness and Orientation of Solution-Grown Silicon Nanowires," *Science* **278**, pp.1471-1473, 2000.
24. K. Peng, J. Hu, Y. Yan, Y. Wu, H. Fang, Y. Xu, S. Lee, and J. Zhu, "Fabrication of Single-Crystalline Silicon Nanowires by Scratching a Silicon Surface with Catalytic Metal Particles," *Adv. Funct. Mater.* **16**, pp.387-394, 2006.
25. M. Tabib-Azar, M. Nassirou, R. Wang, S. Sharma, T. I. Kamins, M. Saif Islam, and R. S. Williams, "Mechanical properties of self-welded silicon nanobridges," *Appl. Phys. Lett.* **87**, pp.113102, 2005.
26. K. Peng, Y. Xu, Y. Wu, Y. Yan, S. T. Lee, and J. Zhu, "Aligned Single-Crystalline Si Nanowire Arrays for Photovoltaic Applications," *Small* **11**, pp.1062-1067, 2005.